

UCSF

UC San Francisco Previously Published Works

Title

Impact of tumor localization on antitumor immunity with conditionally activated CTLA-4 blockade

Permalink

<https://escholarship.org/uc/item/8rp7t2cq>

Journal

Journal for ImmunoTherapy of Cancer, 13(4)

ISSN

2051-1426

Authors

Arias-Badia, Marcel

Pai, Chien-Chun Steven

Lwin, Yee May

et al.

Publication Date

2025-04-01

DOI


10.1136/jitc-2024-010566

Copyright Information

This work is made available under the terms of a Creative Commons Attribution-NonCommercial License, available at <https://creativecommons.org/licenses/by-nc/4.0/>

Peer reviewed

Impact of tumor localization on antitumor immunity with conditionally activated CTLA-4 blockade

Marcel Arias-Badia ¹, Chien-Chun Steven Pai,¹ Yee May Lwin,¹ PeiXi Chen,¹ Aahir Srinath,¹ Miho Tanaka,¹ Emily Musser,² Andrew Goodearl,² Jacob V Gorman,³ Wendy Ritacco,² Lawrence Fong^{1,4}

To cite: Arias-Badia M, Pai C-
CS, Lwin YM, *et al.* Impact of
tumor localization on antitumor
immunity with conditionally
activated CTLA-4 blockade.
*Journal for ImmunoTherapy
of Cancer* 2025;**13**:e010566.
doi:10.1136/jitc-2024-010566

► Additional supplemental
material is published online only.
To view, please visit the journal
online ([https://doi.org/10.1136/
jitc-2024-010566](https://doi.org/10.1136/jitc-2024-010566)).

Accepted 17 March 2025



© Author(s) (or their
employer(s)) 2025. Re-use
permitted under CC BY-NC. No
commercial re-use. See rights
and permissions. Published by
BMJ Group.

¹Department of Medicine,
University of California San
Francisco, San Francisco,
California, USA

²AbbVie Bioresearch Center,
Worcester, Massachusetts, USA
³AbbVie Inc, North Chicago,
Illinois, USA

⁴Immunology Integrated
Research Center, Fred
Hutchinson Cancer Center,
Seattle, Washington, USA

Correspondence to

Dr Lawrence Fong;
lawrence.fong@fredhutch.org

ABSTRACT

Background Immune checkpoint blockade (ICB) can induce antitumor efficacy but also induces immune-related adverse events. Systemically administered ICB can activate immune cells throughout the host. Conditionally active ICB with proteolytically cleaved masking domains can potentially reduce the adverse events seen with anti-cytotoxic T-lymphocyte associated protein 4 (CTLA-4) antibody.

Methods We examined how different formats of a conditionally activated dual variable domain IgG (DVD) that binds CTLA-4 and the tumor-associated antigen prostate stem cell antigen (PSCA) can lead to efficacy in syngeneic subcutaneous and metastatic murine tumor models. We also defined the capacity of these DVDs to modulate immune responses by multiparameter flow cytometry.

Results Conditionally active DVDs can uncouple antitumor efficacy from toxicity. A fully cleavable construct (symmetric DVD, sDVD), which can be released from the target tumor cells, showed superior antitumor efficacy compared with asymmetric DVD, which retains its tumor antigen binding. The sDVD elicited the highest tumor-antigen-specific T-cell responses detected in tumors and tumor-draining lymph nodes, as well as presenting the highest rate of intratumoral and splenic “non-exhausted” antigen-specific CD8 T cells. sDVD also induced the highest degrees of T-cell memory and self-renewal potential. These effects were dependent on PSCA expression by the tumors.

Conclusions These findings support the notion that ICB modulation of antitumor immunity away from the tumor cells is critically important for optimal antitumor immunity. The bispecific sDVD antibody design may enable improved systemic antitumor responses than traditional ICB in both primary tumors and metastases.

BACKGROUND

Immune checkpoint inhibition has revolutionized cancer treatment by stimulating endogenous antitumor T cells. However, immune-related adverse events (irAEs) represent a significant hurdle and are most pronounced with cytotoxic T-lymphocyte associated protein 4 (CTLA-4) blockade alone or in combination with other immunotherapies.^{1,2} These span to many organs—notably

WHAT IS ALREADY KNOWN ON THIS TOPIC

⇒ Systemic immune checkpoint blockade leads to unwanted toxicity in the form of immune-related adverse events.

WHAT THIS STUDY ADDS

⇒ Systemically administered, conditionally activated anti-cytotoxic T-lymphocyte associated protein 4 uncouples toxicity from antitumor efficacy but must not remain localized at the tumor.

HOW THIS STUDY MIGHT AFFECT RESEARCH, PRACTICE OR POLICY

⇒ Conditional activation of immune checkpoint inhibitors can improve the therapeutic index of cancer immunotherapy.

the gastrointestinal (GI) tract, skin and kidneys—and can be life-threatening, implying the interruption of the cancer therapy or the incorporation of immunoinhibitory treatments that dampen the effect of anticancer immune checkpoint blockade (ICB). In a recent clinical trial in patients with prostate cancer treated with ICB, one-third of them presented grade 3–4 treatment-related adverse events.³ In the case of ipilimumab, a successful anti-CTLA-4 (aCTLA-4) antibody, the majority of patients (>70%) present some degree of dose-dependent irAE.⁴ In some malignancies, local administration might alleviate these events at the expense of notable technical challenges.^{5,6} We previously demonstrated that antitumor efficacy could be uncoupled from immune-related damage in non-tumoral tissues by the conditionally activated dual variable domain (DVD) bispecific antibodies, where masking domains blocking aCTLA-4 binding are cleaved by membrane type-serine protease 1 or matrilysin (MT-SP1), which is overexpressed in the tumor microenvironment (TME).⁷ In this study, we examined whether confining the

unmasked aCTLA-4 to the TME had an impact on anti-tumor immunity. We studied two architectures of prostate stem cell antigen-(PSCA) targeted CTLA-4 antibodies: a symmetric DVD (sDVD), where the heavy and light chain linkers of both anti-PSCA domains are cleaved releasing a functionalized aCTLA-4 antibody that can diffuse away, and an asymmetric DVD antibody (aDVD), where only the heavy chain linker is cleavable in each anti-PSCA domain, leading to an aCTLA-4 antibody that remains tethered to target cells after activation. DVD molecules present a slight increase in molecular weight of around 1.3-fold compared with native aCTLA-4, but their binding and pharmacodynamic properties remain at comparable levels to native aCTLA-4.⁷ We validated the safety of linker cleavage and primary target binding of these molecules in unleashing aCTLA-4 activity with relevant uncleavable DVD (unDVD) and irrelevantly tetanus-toxin targeted DVD (ttDVD) controls. We also show that sDVD is able to optimally control PSCA⁺ prostate TRAMP-C2 and colorectal MC38 tumor growth without compromising safety and, surprisingly, induce protective systemic immune effects that do not entail unwanted immune overaction, while having isotype-comparable effects in PSCA⁻ tumors. Our findings demonstrate the importance of regional exposure to ICB in improving clinical efficacy while limiting adverse events.

RESULTS

Conditionally activated DVDs uncouple efficacy from body weight loss in localized tumors

To study whether tumor localization of ICB impacts anti-tumor efficacy, we compared an aDVD antibody that would remain constitutively tethered to the target PSCA⁺ cells with a fully cleavable sDVD antibody (sDVD) in the syngeneic PSCA⁺ TRAMP-C2 murine prostate tumor model (figure 1A–B). In these experiments, we also tested the importance of tumor targeting and activation with an aCTLA-4 DVD targeting tetanus toxoid (ttDVD, a molecule we consider non-targeted in mice), a DVD with uncleavable scrambled linkers (unDVD), and the native aCTLA-4 antibody (figure 1C). The sDVD had nearly identical antitumor activity and survival rates compared with native aCTLA-4 (average 565 and 634 mm³, both with 37% survival by day 120 post-enrollment, respectively), while the tethered aDVD treatment trended toward inferior tumor growth control and survival (figure 1D–E). No treatment-induced weight loss was observed with any DVD construct, while aCTLA-4 induced moderate weight loss by day 18 after treatment, at a time when tumor volumes would not confound body weight measurements (figure 1F). While we confirmed previously reported increased CD8⁺ infiltration in DVD-treated tumors, increased effector CD8⁺ T-cell frequencies were also observed in tumor-draining lymph nodes (TDLN) of these mice, suggesting ongoing T-cell expansion following systemic antitumor responses (figure 1G). Across experiments, sDVD treatment led to 40% tumor-free animal rates, on par with native aCTLA-4,

while aDVD only showed a 25% overall tumor-free rate. These results underscore the combination of systemic availability with conditional activation as features for optimal ICB responses. sDVD uncouples efficacy from irAEs in disseminated tumors

Next, we examined the efficacy of DVDs against disseminated tumors as a model of metastasis. We used murine MC38 cells either transduced with murine PSCA or with an empty vector (EV) (figure 2A–B, online supplemental figure 2). Tumor cells were injected intravenously and treatment was initiated 7 days later with sDVD or aCTLA-4 (online supplemental figure 2). Tumor growth was then monitored by *in vivo* bioluminescence (figure 2A–B). sDVD induced significant antitumor activity against PSCA⁺ MC38 at a similar magnitude as aCTLA-4, but without causing weight loss (figure 2C–F, online supplemental figure 2). We analyzed the GI tract of mice harboring PSCA⁺ tumors as a clinically relevant organ where ICB-related adverse events occur in responding patients, and found a nominal trend for higher total CD4⁺ T counts as well as higher expression of tumor necrosis factor- α in aCTLA-4-treated mice compared with the other groups (figure 2G–H and online supplemental figure 2). Macroscopic examination of mice during these experiments revealed a higher occurrence of events decreasing body conditioning score in aCTLA-4-treated animals such as hair loss, squinted eyes or affected mobility, as well as rare cases of dermatitis or anal inflammation (n=1) not observed in the other treatment groups (online supplemental figure 2). Unlike aCTLA-4, sDVD was not efficacious in PSCA⁻ MC38 tumors, confirming the requirement for tumor antigen targeting to optimally activate the conditional DVD. sDVD enhances immune responses in disseminated tumors

We then defined the treatment-induced immune response within the lung metastasis. At day 15 post-tumor injection, sDVD treatment induced the highest CD8⁺ infiltration in PSCA⁺ lung tumors, nearly doubling that seen for aCTLA-4 in either PSCA⁻ or PSCA⁺ tumors (figure 3A). sDVD treatment depleted regulatory FoxP3⁺ CD4⁺ T cells (regulatory T cell (Treg)) in lungs implanted with PSCA⁺ tumors, consistent with known Treg-depleting effects of native aCTLA-4 antibodies (3) (figure 3B). We found increases in effector memory CD44⁺CD62L⁻ T cells in the three responding groups (figure 3C). In terms of tumor antigen-reactive CD8⁺ T cells, we found that sDVD treatment led to superior induction of CD8⁺ ADPGK-reactive T cells⁸ in PSCA⁺ tumors, again doubling the frequency of these cells compared with aCTLA-4 treatment (figure 3D–E), consistent with the localized TRAMP-C2 model. Again, the effect of antitumor T-cell induction required PSCA expression with the sDVD, but not with aCTLA-4. Apdkg-reactive T cells from sDVD-treated tumors showed the highest levels of perforin and Ki67 expression (figure 3F and G). sDVD treatment induced comparable levels to aCTLA-4 treatment of PD-1⁺ TCF-1⁺ progenitor exhausted T cells (Tpex) (figure 3H). We also interrogated the exhaustion status of

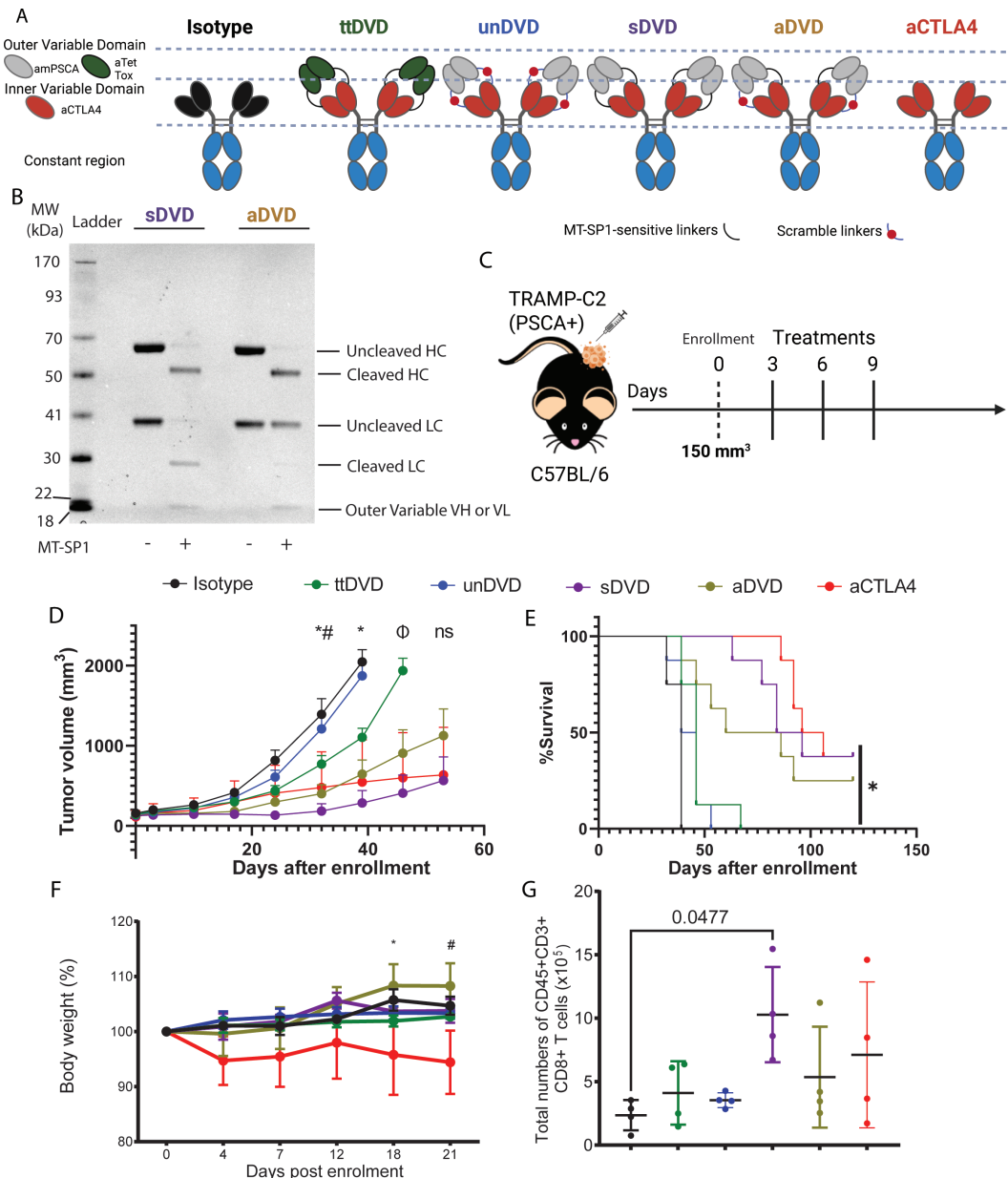


Figure 1 DVD anti-CTLA-4 shows specific, safe antitumor efficacy in murine subcutaneous PSCA⁺ tumors. (A) Antibodies used in subcutaneous tumor experiments. In DVD antibodies (untargeted: ttDVD; uncleavable: unDVD; symmetric: sDVD; asymmetric: aDVD), tissue specificity is conferred by murine PSCA targeting in the outer variable domain. On tumor-induced upregulation of matriptase (MT-SP1), the linkers between both variable domains are cleaved and the CTLA-4-targeting inner variable domains are exposed and functional. (B) Uncleaved and matriptase-cleaved sDVD and aDVD resolved in 4–12% gradient SDS-PAGE gel. Briefly, 20 μ g of each antibody were incubated overnight in the presence of 5 μ L (2.5 μ g) recombinant matriptase at room temperature. 3 μ g of lysate were loaded onto SDS-PAGE gels and protein content was detected by SafeBlue staining. (C) Experiment design for the assessment of the antitumor efficacy of the DVD anti-CTLA-4 antibodies. 1 million mouse prostate TRAMP-C2 tumor cells were implanted on the right flanks of C57BL/6J mice ($n=5-8$). When tumors reached 150 mm³ (day 0), mice were enrolled into treatment groups, and injected intraperitoneally with antibodies on days 3, 6 and 9. Tumor growth was monitored twice weekly. (D) Tumor volume curves for mice ($n=7-8$ per group) from $n=1$ of three experiments in (C). * $p<0.05$ sDVD versus: isotype, unDVD; #, $p<0.05$ aDVD versus: isotype, unDVD; Φ , $p<0.05$ sDVD, aCTLA-4 versus ttDVD. One-way analysis of variance applying Kruskal-Wallis test was used for all shown p values. Error bars represent SEM. (E) Kaplan-Meier survival curves for mice ($n=7-8$ per group) from $n=1$ of three experiments in (C). * $p<0.05$ aCTLA-4, sDVD and aDVD versus rest by log-rank Mantel-Cox test. (F) Percentage of body weight variation for mice ($n=7-8$ per group) from $n=1$ of three experiments in (C). Error bars represent SEM. * $p<0.05$ aCTLA-4 versus isotype, aDVD; # $p<0.05$ aCTLA-4 versus isotype, unDVD, sDVD and aDVD. (G) Total gated CD45⁺ CD3⁺ CD8⁺ T-cell counts from lymph nodes of mice ($n=4$ from $n=1$ of three experiments) involved in (C) by flow cytometry. aCTLA-4, anti-cytotoxic T-lymphocyte associated protein 4; DVD, dual variable domain; HC, heavy chain; LC, light chain; MW, molecular weight; PSCA, prostate stem cell antigen; SDS-PAGE: Sodium dodecyl-sulfate polyacrylamide gel electrophoresis; VH: variable domain of the heavy chain; VL, variable domain of the light chain; ttDVD, tetanus-toxin targeted DVD.

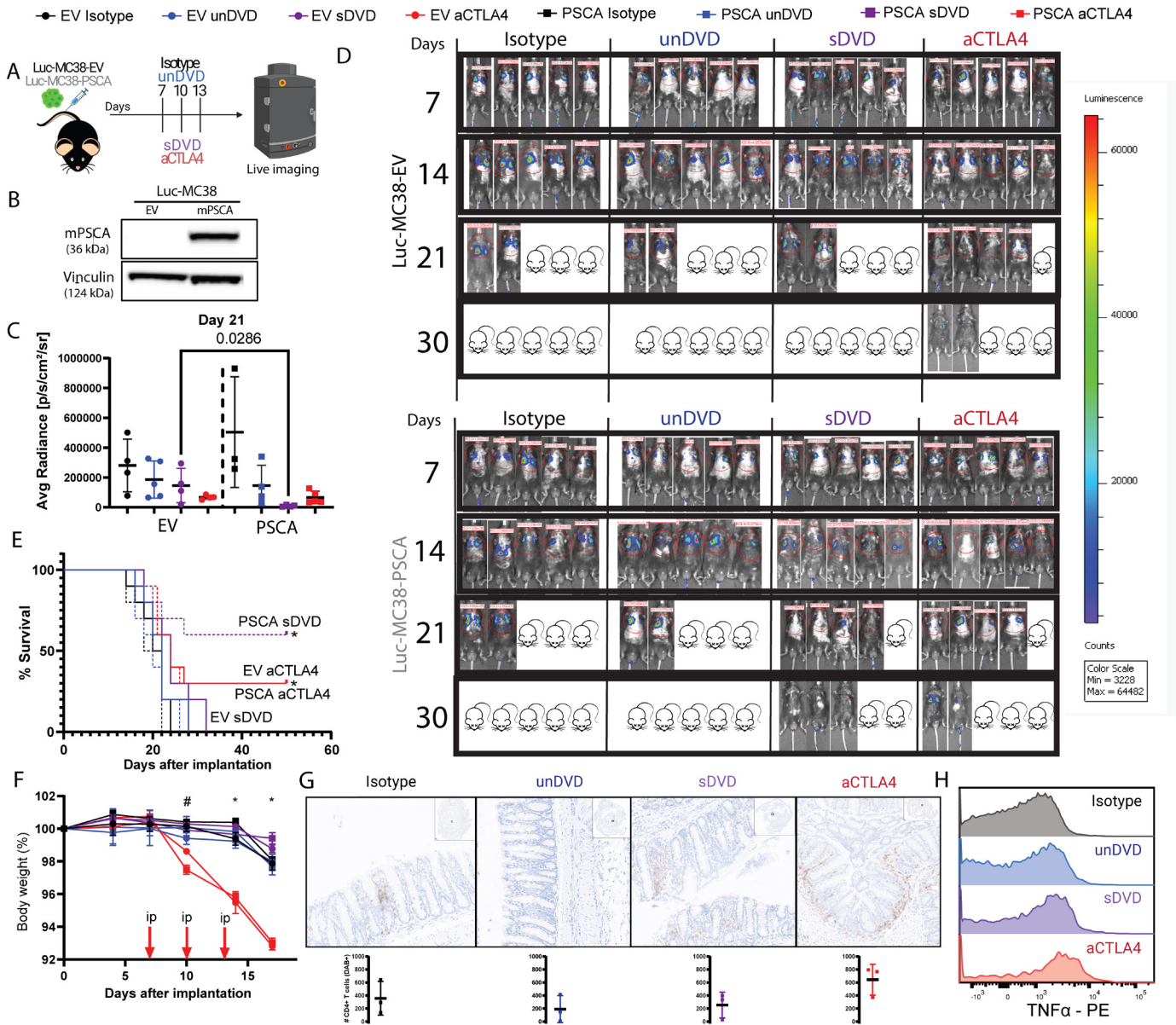


Figure 2 PSCA-targeted anti-CTLA-4 shows specific antitumor efficacy in systemic PSCA⁺ tumors. (A) Experiment summary for characterization of PSCA⁺ MC38 cells. Briefly, luciferase-expressing empty vector (EV) PSCA⁻ or PSCA⁺ MC38 cells were injected intravenously in C57BL/6J mice (n=5 per group). Treatment was administered intraperitoneally on days 7, 10 and 13 after implantation. Tumor growth was monitored by in vivo luminescence quantification twice a week. (B) Murine PSCA (mPSCA) expression on Luc-MC38 cell lines by western blot. (C) In vivo bioluminescence quantification of luciferase-expressing MC38 cells in mice (n=4) from n=1 of two experiments described in (A) on day 21 after tumor cell injection, shown as average photon radiance. (D) Representative individual whole-body images of mice from n=2 experiments involved in (A) on days 7, 14, 21 and 30 after systemic tumor implantation, colored by tumor luminescence intensity. Red circles are regions of interest (ROIs) considered for bioluminescence quantification with Living Image Software. Total photon counts are shown above ROIs. Mouse drawings with crossed eyes represent the percentage of deceased mice for each group (20% each). (E) Kaplan-Meier survival curves for mice (n=10) involved in (A) (n=2 experiments). *p<0.05 versus EV isotype, EV sDVD, EV unDVD, mPSCA isotype, mPSCA unDVD by log-rank Mantel-Cox test. (F) Percentage of body weight variation for mice (n=10) involved in (A) (n=2 experiments). Error bars represent SEM. *p<0.05 EV aCTLA-4, PSCA aCTLA-4 versus rest; # p<0.05 EV aCTLA-4 versus EV sDVD, PSCA isotype by one-way analysis of variance. (G) GI tracts from animals (n=3) harboring PSCA⁺ tumors from n=1 experiment were stained for CD4. For each experimental group, a representative ROI is shown on top, and DAB⁺ (CD4⁺) counts below. (H) Mean fluorescence intensity offset histograms of TNF- α in GI-derived CD4⁺T cells from PSCA⁺-challenged mice by flow cytometry. aCTLA-4, anti-cytotoxic T-lymphocyte associated protein 4; DVD, dual variable domain; GI, gastrointestinal; mPSCA, murine prostate stem cell antigen; PE, phycoerythrin; sDVD, symmetric DVD; TNF, tumor necrosis factor; unDVD, uncleavable DVD.

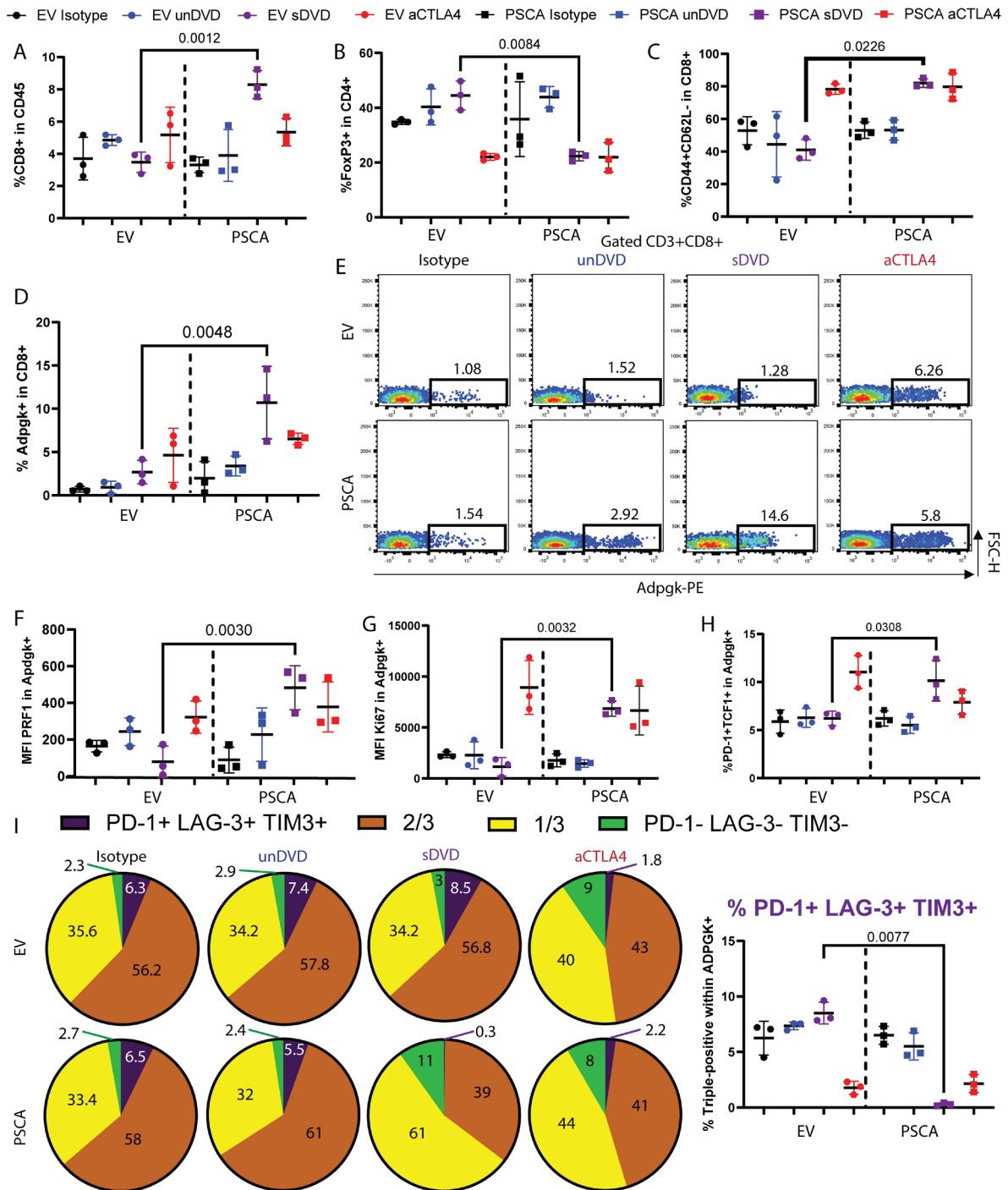


Figure 3 PSCA-targeted DVD anti-CTLA-4 induces antigen-specific responses and improved T-cell fitness in systemically implanted PSCA⁺ tumors. (A) Percentage of CD8⁺ T cells within the immune CD45⁺ compartment from flow cytometry data from lung tumors of mice (n=3) harvested on day 15 after tumor injection. As in the rest of the figure, representative data from n=1 of two experiments is shown. (B) Percentage of intratumoral FoxP3⁺ cells within gated CD4⁺ T cells. (C) Percentage of intratumoral CD44⁺ CD62L⁻ cells within gated CD8⁺ T cells. (D) Percentage of intratumoral MC38 antigen-specific ADPGK-reactive CD8⁺ T cells. (E) Representative flow cytometry pseudocolor dot plots showing MC38 antigen ADPGK reactivity in gated CD8⁺ T cells from mouse lung tumors. Shown values are percentages within all CD8⁺. (F) MFI of effector molecule perforin (PRF1) in intratumoral ADPGK⁺ CD8⁺ T cells. (G) MFI of proliferation marker Ki67 in gated intratumoral ADPGK⁺ CD8⁺ T cells. (H) Percentage of PD-1⁺ TCF1⁺ cells in gated intratumoral ADPGK⁺ T cells. (I) Part-of-whole pie charts showing mean percentages of cells expressing 0, any given 1, any combination of 2, or 3 exhaustion markers PD-1, LAG-3, TIM3 in intratumoral ADPGK⁺ CD8⁺ T cells, as assessed by Boolean gating from flow cytometry data. Right, percentage of intratumoral PD-1⁺ TIM3⁺ LAG-3⁺ in ADPGK⁺ CD8⁺ T cells. aCTLA-4, anti-cytotoxic T-lymphocyte associated protein 4; DVD, dual variable domain; EV, empty vector; LAG-3, lymphocyte-activation gene 3; MFI, mean fluorescence intensity; PD-1, programmed cell death protein 1; PSCA, prostate stem cell antigen; sDVD, symmetric DVD; unDVD, uncleavable DVD; TIM3, T-cell immunoglobulin and mucin-domain containing-3.

ADPGK-reactive CD8⁺ T cells by quantifying simultaneous expression of PD-1, TIM3, and LAG-3. Correlating again with response rates, the percentage of PD-1⁻ TIM3⁻ LAG-3⁻ (triple-negative) T cells was highest in sDVD treatment from PSCA⁺ tumors (11%) and both aCTLA-4-treated groups (9%), whereas PD-1⁺ TIM3⁺ LAG-3⁺ T cells were lowest in these groups (figure 3I and online supplemental table 1). Notably, these differences in phenotype on the ADPGK-reactive T cells were absent with sDVD treatment in PSCA⁻ tumors. Altogether, these findings confirm the improved T-cell fitness resulting from treatment with sDVD.

sDVD modulates systemic immunity

To characterize systemic effects of the DVD aCTLA-4 therapy, we also examined T-cell responses in the spleen and TDLNs of treated mice. While overall circulating CD4⁺ T-cell frequencies were unchanged in treated mice (figure 4A) and no significant differences were found in the weight of either organ (online supplemental figure 4), we observed a moderate decrease in circulating Tregs, combined with significantly increased CD44⁺CD62L⁻ effector memory CD4⁺ T cells in mice harboring PSCA⁺ tumors treated with sDVD (figure 4B–C). Similarly, although overall CD8⁺ frequencies remained unaltered in all experimental groups (figure 4D), there was a significant increase in the frequency of circulating ADPGK-reactive CD8⁺ T cells (0.6–1% of CD8⁺ T cells) in mice treated with aCTLA-4, as well as in spleens from mice harboring PSCA⁺ tumors treated with sDVD (figure 4E–F), consistent with a systemic expansion of tumor-reactive T cells. These circulating tumor antigen-specific T cells showed significantly higher levels of perforin and Ki67, in line with increased cytolytic and proliferative capability, respectively (figure 4G–H). We also found increased frequencies of circulating PD-1⁺TCF1⁺ TpeX ADPGK-reactive T cells in mice harboring PSCA⁺ tumors treated with sDVD (up to 19.7%) and aCTLA-4 (up to 20.6%) (figure 4I). ADPGK-reactive CD8⁺ T cells expressing at least one marker of T-cell exhaustion were enriched in mice harboring PSCA⁺ tumors treated with sDVD compared with PSCA⁻ tumors, suggesting antigen specificity, while PD-1⁻ TIM3⁻ LAG-3⁻ cells were highest (46%) in spleens from sDVD-treated, PSCA⁺ tumor-challenged mice among all responding groups. Parallel trends were observed for aCTLA-4-treated mice in both tumor types, with significant differences observed in this group against non-responding unDVD-treated PSCA⁺ tumor-challenged mice. Terminally exhausted T cells simultaneously expressing PD-1, LAG-3 and TIM3 were not observed in circulation in any experimental group (figure 4J and online supplemental table 1). Finally, ADPGK-reactive T-cell frequencies were highest in TDLNs from mice harboring PSCA⁺ tumors treated with sDVD, accounting for up to 8.3% of all CD8⁺ T cells, while sDVD treatment did not have detectable expansion in TDLNs from mice harboring PSCA⁻ tumors. In contrast, treatment with aCTLA-4 led to significantly elevated ADPGK-reactive

frequencies in TDLNs regardless of PSCA expression (figure 4K–M). Altogether, these findings underscore how conditional DVDs can restrict immunomodulation in an antigen-specific fashion, allowing for effective systemic antitumor responses at comparable levels to traditional ICB without eliciting unwanted toxicities.

DISCUSSION

Systemic delivery of ICB is associated with systemic immune activation and toxicities.^{19,10} In order to circumvent this, some have proposed intratumoral or peritumoral delivery of minimal doses of aCTLA-4 both in preclinical and clinical cancer settings.^{5,11–16} While intratumoral administration of immunotherapies reduces drug dosage considerably and has been shown to induce antitumor responses, these often are local and may be of limited utility in the metastatic setting.¹⁷ Nevertheless, systemic immune responses have been shown to be critical for effective antitumor activity on treatment with ICB,^{18–20} which motivates the development of engineered immunotherapies that are systemically delivered but conditionally activated in the TME.^{21,22} We have previously demonstrated the safety of DVD-based aCTLA-4 therapy⁷; however, the critical features of these molecules are yet to be defined. In this study, we find that confining the aCTLA-4 activity to the tumor cells with the constitutively tethered aDVD may compromise the efficacy and immune responses induced, indicating that CTLA-4 blockade beyond the TME also plays an important role, both in localized and disseminated tumor models. Another intriguing observation is the dependence of the DVD tumor antigen targeting domain: we saw no antitumor activity against PSCA⁻ tumors. Most of the ongoing conditionally activated immunotherapies in the clinic do not have a targeting domain and yet are activated by proteases in the TME of solid tumors, as in the primary or metastatic castration-resistant prostate cancer trial NCT05519449, or the NCT05479812 and NCT06462794 trials targeting multiple tumor types. With our DVD, PSCA binding may enhance protease access to the cleavage domains, perhaps through greater dwell time in the TME or conformational change, which could be examined in future work. Nevertheless, DVDs enable an additional level of tumor specificity.

While sDVD induces Treg depletion seen with conventional aCTLA-4 antibody treatment,^{23,24} our study shows a significant boost of tumor antigen-reactive CD8⁺ T cells⁸ that possess improved immune fitness as reflected by their elevated expression of cytolytic perforin, increased proliferation, and reduced expression of exhaustion markers. These data underscore the synergistic dual effect—Treg depletion and antigen-responsive T-cell reinvigoration—of aCTLA-4 therapy suggested by others.²⁵ Moreover, we also saw an increased PD-1⁺ TCF-1⁺ TpeX, thought to be drivers of antitumor T-cell renewal on ICB treatment.^{26,27} Our analysis of lymphoid organs revealed a systemic marker of response to ICB in the form of

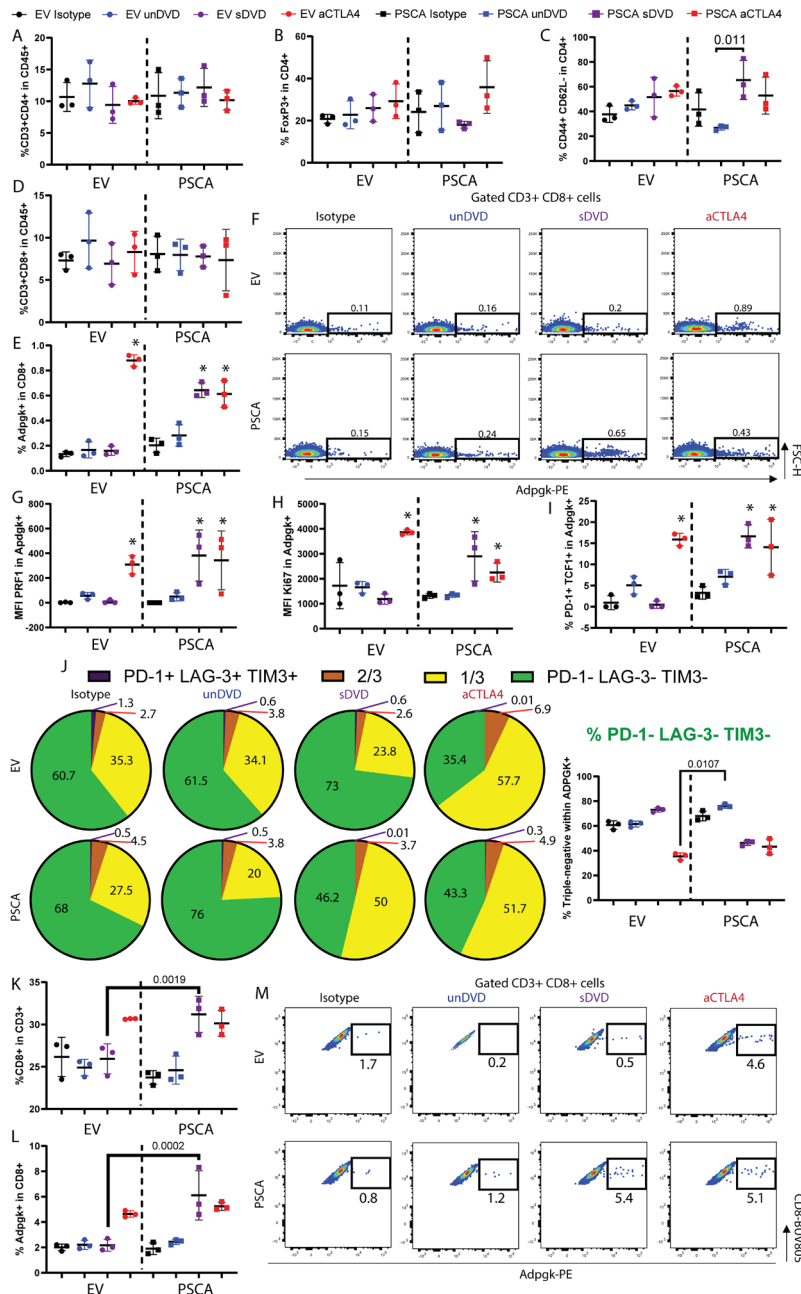


Figure 4 Symmetric DVD induces systemic immune responses. (A) Percentage of CD4⁺ T cells within the immune CD45⁺ compartment from flow cytometry data from spleens of mice (n=3) harvested on day 15 after tumor injection. As in the rest of the figure, representative data from n=1 of two experiments is shown. (B) Percentage of FoxP3⁺ cells within gated CD4⁺ T cells. (C) Percentage of CD44⁺ CD62L⁻ cells within gated CD4⁺ T cells. (D) Percentage of splenic CD8⁺ T cells within the immune CD45⁺ compartment. (E) Percentage of splenic MC38 antigen-specific ADPGK-reactive CD8⁺ T cells. Shown p values obtained by one-way analysis of variance adjusted for multiple comparisons; *p<0.05 versus rest. (F) Representative flow cytometry pseudocolor dot plots showing MC38 antigen ADPGK reactivity in gated CD8⁺ T cells from mouse spleens. Shown values are percentages within all CD8⁺. (G) MFI of effector molecule perforin (PRF1) in gated splenic ADPGK⁺ CD8⁺ T cells. *p<0.05 versus rest. (H) MFI of proliferation marker Ki67 in gated splenic ADPGK⁺ CD8⁺ T cells. *p<0.05 versus rest. (I) Percentage of PD-1⁺ TCF1⁺ cells in gated splenic ADPGK⁺ CD8⁺ T cells. *p<0.05 versus rest. (J) Part-of-whole pie charts showing mean percentages of cells expressing 0, any given 1, any combination of 2, or 3 exhaustion markers PD-1, LAG-3, TIM3 in splenic ADPGK⁺ CD8⁺ T cells, as assessed by Boolean gating from flow cytometry data. Right, percentage of splenic PD-1⁻ TIM3⁻ LAG-3⁻ in ADPGK⁺ CD8⁺ T cells. (K) Percentage of CD8⁺ T cells within the immune CD45⁺ compartment in mouse tumor-draining lymph nodes (TDLNs). (L) Percentage of MC38 antigen-specific ADPGK-reactive CD8⁺ T cells in TDLNs. (M) Representative flow cytometry pseudocolor dotplots showing MC38 antigen ADPGK reactivity in gated CD8⁺ T cells from mouse TDLNs. Shown values are percentages within all CD8⁺. aCTLA-4, anti-cytotoxic T-lymphocyte associated protein 4; DVD, dual variable domain; EV, empty vector; LAG-3, lymphocyte-activation gene 3; MFI, mean fluorescence intensity; PD-1, programmed cell death protein 1; PSCA, prostate stem cell antigen; sDVD, symmetric DVD; unDVD, uncleavable DVD; TIM3, T-cell immunoglobulin and mucin-domain containing-3.

increased non-exhausted (TIM3⁻LAG3⁻) splenic and lymph node ADPGK⁺ CD8⁺ T-cell frequencies that maintained their cytotoxic, proliferative and antigen experience features, suggesting readiness against disseminated disease. While overall responses at the cellular and proteomic level were not immensely different between sDVD and regular aCTLA-4, the lack of toxicity combined with the improved survival on DVD treatment suggest a more optimal availability of therapeutic molecules from a tissue-specific treatment such as DVD, which would be critical to ascertain in future studies. These findings not only confirm the specificity and safety of the DVD technology, but also pose tissue-activatable ICB leading to systemic responses like the ones elicited by sDVD as advantageous compared with toxic, indiscriminate systemic ICB (aCTLA-4), or more invasive, sometimes impractical intratumorally delivered ICB. More studies focusing on pharmacodynamics and potential loss of functional molecules in the latter could reveal exploitable avenues to improve cancer immunotherapy mediated by checkpoint inhibition.

Our study has some limitations. First, while we were able to characterize immune responses on DVD treatment in PSCA⁻ and PSCA⁺ versions of the same tumor model, additional systemically implanted tumor types—ideally with endogenous expression levels of the target antigen—would validate the antitumor advantage of DVD in physiologically relevant levels of antigen, as well as its associated expansion of other antigen-specific T-cell responses. While we studied the prostate subcutaneous TRAMP-C2, which expresses endogenous levels of PSCA, this tumor line did not generate tumors on systemic implantation. While we previously demonstrated the safety of the DVD platform in relevant preclinical models,⁷ further comprehensive pharmacodynamic and bioavailability characterization of sDVD, aDVD and native aCTLA-4 alongside multiorgan pathological analysis could help expand our understanding of the uncoupling of toxicity and efficacy observed in this study, which was limited to body weight monitoring and statistically constrained analysis of the GI in mice challenged with PSCA⁺ tumors. Finally, additional studies could examine whether heterogeneous expression of the DVD target antigen (PSCA in this case) represents a potential mechanism of immune escape. If ICB is able to enlist the endogenous T-cell repertoire to target heterogeneous tumors, this may not be an issue. This would broaden the potential pool of targeting antigens for DVD-based antibodies.

Overall, the fully cleavable sDVD aCTLA-4 antibody described in this study was able to promote antigen-specific T-cell expansion, effector and self-renewing tumor-infiltrating T-cell phenotypes, as well as to improve outcomes in mice harboring metastatic MC38 tumors without showing safety concerns. Our findings demonstrate the importance of not just targeting an immunotherapy to the TME but also having some regional exposure, presumably including the tumor training lymph nodes, where we now appreciate ICB responses

that are T_{PEX}-resided.¹⁹ This leakiness will need to be considered in developing future bispecific or conditional immunotherapies.

METHODS

Anti-CTLA-4 antibodies

The mouse aCTLA-4 (clone 24H2) and all DVD antibodies were generated by AbbVie (Chicago, USA) as described previously.⁷ Briefly, the mouse symmetric aCTLA-4 DVD antibody (sDVD) contains MT-SP1-cleavable linkers at either side of the Fab fragment, whereas the aDVD antibody contains those linkers only in one of its variable chains. The untargeted DVD antibody (ttDVD) targets Tetanus toxin instead of murine PSCA and contains MT-SP1-cleavable linkers. The unDVD antibody targets murine PSCA and contains scrambled linkers uncleavable by MT-SP1.

Matriptase cleavage and SDS-PAGE

Degree of cleavage of DVD antibodies sDVD and aDVD was assessed by overnight incubation of 20 µg of each in the presence of 5 µL recombinant Matriptase (3946-SEB-010, BioTechne) at room temperature. Then, 3 µg lysates were prepared in NuPAGE LDS Sample Buffer (NP0007, Invitrogen), loaded onto 4–12% Bis-Tris NuPAGE gels (NP0322BOX, Invitrogen) and gel electrophoresis was run in MOPS buffer (NP0001, Invitrogen), after which protein content was stained with SimplyBlue SafeStain (LC6065, Invitrogen) following the manufacturer's protocol. 3 µg uncleaved sDVD and aDVD were added in parallel to the Sodium Dodecyl Sulfate Polyacrylamide Gel Electrophoresis (SDS-PAGE) gels. SeeBlue Protein Ladder (LC5925, Invitrogen) was run for molecular weight reference.

Animal studies, cell lines and in vivo imaging

8–10-week-old male WT C57BL/6J mice (000664, Jackson) were used in mouse experiments described in this study. All experiments performed were reviewed and approved by the Institutional Animal Care and Use Committee (IACUC) at University of California, San Francisco (UCSF) under protocol number AN202446. For in vivo tumor studies, 1 million murine prostate adenocarcinoma TRAMP-C2 cells were injected subcutaneously on the right flank of mice (n=5–8 per group). For systemic tumor experiments, 5×10⁵ murine colorectal carcinoma MC38 cells (CVCL_B288) were injected intravenously through the tail vein of each animal (n=5 per group) on day 0. On day 7 after implantation, animals were fully randomized into groups and treated intraperitoneally (i.p.) on days 3, 6 and 9 with isotype IgG2a/k control, aCTLA-4 (clone 24H2, AbbVie), control or functional DVD antibodies (AbbVie). In subcutaneous implantation studies, tumors were measured twice a week with a digital caliper (Fisher). Tumor volume was obtained with the formula $V=L(\text{length})\times W(\text{width})\times W\times\pi/6$, where L was the higher measure, and W was the lower measure. Endpoint

Table 1 Antibodies used in flow cytometry

Marker	Conjugation	Vendor	Catalog #	Clone
CD45	PB	BioLegend	103126	30-F11
CD8 α	BUV805	BD	612898	53-6.7
CD4	BV711	BioLegend	100447	GK1.5
CD3	BUV395	BD	563565	145-2C11
PD-1	PE-Dazzle594	BioLegend	109115	RMP1-30
H-2Db ADPGK ASMTNMELM	PE	MBL	TB-5113-1	N/A
PRF1	APC	BioLegend	154303	S16009A
Ki-67	BV480	BD	566109	B56
FoxP3	PE-Cy7	LT	25-5773-80	FJK-16s
TCF-1	A488	BD	567018	S33-966
TIM3	PerCP-Cy5.5	BioLegend	134012	B8.2C12
LAG-3	BV785	BioLegend	125219	C9B7W
CD44	BV650	BioLegend	103049	IM7
CD62L	BV570	BioLegend	104433	MEL-14
TNF- α	PE	BioLegend	506305	MP6-XT22

was set at 2,000 mm³. In systemic implantation studies, tumor progression was monitored using an IVIS Spectrum in vivo imaging device (Xenogen) until day 25, after which survival was monitored. Endpoint was set at Body Condition Scoring of ≤ 2 . Briefly, animals were injected i.p. with 0.2 mL of Dulbecco's Phosphate Buffered Saline (DPBS) containing 3 mg D-Luciferin (88294, Thermo) and were imaged after a 3 min incubation. Images were processed and bioluminescence radiance was quantified using the Living Image Software, V.4.7.4.20726. All mice were maintained at the UCSF vivarium at all times and received food and water ad libitum. Experiment performers were not blinded to experimental conditions, but randomization was done on a “per animal” basis, and not “per cage”.

Generation of Luc-MC38 cells expressing murine PSCA

Luciferase-expressing mouse colorectal adenocarcinoma MC38 cells were kindly provided by Jeff Bluestone (UCSF, San Francisco, USA). For the generation of the Luc-MC38-PSCA cell line, an insert containing the murine PSCA complementary DNA sequence 5'-A T G A A G A C C G T C T T C T T T C T C C T G C T G G C C A C C T A C T T A G C C C T G C A T C C A G G T G C T G C T C T G C A G T G C T A T T C A T G C A C A G C A C A G A T G A A C A A C A G A G A C T G T C T G A A T G T A C A G A A C T G C A G C C T G G A C C A G C A C A G T T G C T T T A C A T C G C G C A T C C G G G C C A T T G G A C T C G T G A C A G T T A T C A G T A A G G G C T G C A G C T C A C A G T G T G A G G A T G A C T C G G A G A A C T A C T A T T T G G G C A A G A A G A A C A T C A C G T G C T G C T A C T C T G A C C T G T G C A A T G T C A A C G G G G C C C A C A C C C T G A A G C C A C C C A C C A C C C T G G G G C T G C T G A C C G T G C T C T G C A G C C T G T T G C T G T G G G G C T C C A G C C G T C T G T A G -3' and flanked by 5' XhoI

(CTCGAG) and 3' SacII (CCGCGG) sites was cloned after restriction enzyme digestion for 2 hours at 37°C into the MSCV2.3 vector, a modified version of MSCV 2.2-IRES2-EGFP (obtained from Lewis Lanier at UCSF, San Francisco, USA). HEK293T cells were transfected with MSCV2.3, along with the Gag/Pol and VSV-G retroviral vector system, in the presence of Lipofectamine 3000 (L3000001, Invitrogen). After 48 hours, HEK293T supernatants containing empty or PSCA—MSCV2.3 retroviral particles were obtained and mixed with 1×10^5 Luc-MC38 cells. Cells were seeded into 6-well plates and incubated at 37°C for 72 hours. CFP⁺ cells were then sorted by flow cytometry, expanded and viably frozen. Luc-MC38-PSCA cells were validated by insert PCR amplification and analysis at TapeStation 4150 (Agilent) and by Sanger sequencing through GeneWiz (Azenta). Primers used for validation were CMVF 5'-TGTACGGTGGGAGGTCTA-3' and IRESR 5'-GACAAACGCACACCGGCCT-3'.

Western blot

Murine PSCA expression was assessed by protein western blot in parental and transfected cells used in animal studies. Cell culture extracts from TRAMP-C2, Luc-MC38, Luc-MC38-EV and Luc-MC38-mPSCA were quantified for protein content with the Pierce BCA Assay Kit (23225, Thermo). Protein lysates (25 μ g protein) were loaded onto pre-made MiniProtean TGX 7.5% PA gels (456–1023, Bio-Rad) and run by electrophoresis. Semi-dry transfer onto a Polyvinylidene fluoride or polyvinylidene difluoride (PVDF) membrane was then performed on a Transblot SD unit (170-3940, Bio-Rad). Membranes were blocked and then incubated overnight at 1:1,000 with anti-mouse PSCA (17171-1-AP, Proteintech) or 1:10,000 anti-vinculin (AB129002, Abcam) as loading control in TBS-T (170-6435, Bio-Rad). After three rounds of washing, membranes were incubated with 1:2,000 secondary HRP

antibody (AB205718, Abcam). After a short incubation with SuperSignal West Pico PLUS Chemiluminescent substrate (34577, Thermo), membranes were imaged with a Chemidoc XRS⁺ (Bio-Rad). Images were initially processed with Image Lab (Bio-Rad) and later prepared for publication with ImageJ (Fiji).

Tissue processing

Lungs, spleens, mediastinal TDLNs from all groups and GI tracts from mice harboring PSCA+ tumors were surgically removed from mice (n=3 per group) with sterilized equipment on day 15 after tumor implantation. Lungs were perfused with phosphate-buffered saline (PBS) and mechanically dissociated with scalpel blades. GI tracts from the n=1 experiment were flushed and washed entirely with PBS to remove inner content and separated into two pieces, one for flow cytometry and one for immunohistochemistry (IHC), which was rolled and placed onto a cassette. For IHC experiments, 5 µm-thick paraffin-embedded slides were prepared from harvested GI tracts. Tissue slides were dehydrated in a battery of incubations in xylene, 100%, 95%, 70% and 50% ethanol. Dehydrated slides were submitted for CD4 staining (AB183685, Abcam) to the UCSF Histology&Biomarker Core at Mt Zion (San Francisco). Full-slide images and representative regions of interest (ROIs) were obtained with ImageScope (Aperio) and further processed with StrataQuest V.5.0 to quantify 3, 3'-diaminobenzidine positive counts (n=5 ROI/mouse). For flow cytometry experiments, lungs and GI tracts were digested to single-cell suspensions by incubation for 1 hour at 37°C in tumor digestion media containing Dulbecco's Modified Eagle Medium (DMEM), 10% Fetal Bovine Serum (FBS), 2 mg/mL Collagenase IV (C5138, Sigma-Aldrich) and DNase I (D5025, Sigma-Aldrich). Spleens and lymph nodes were mechanically dissociated on ice. Tissue lysates were filtered through a 100 µm filter into 50 mL conical tubes and filled with cold PBS, followed by centrifugation at 450 g for 5 min at 4°C. Supernatants were discarded and pellets from lungs and spleens were resuspended in 5 mL ACK Lysing Buffer (118-156-101, Quality Biological), mixed well and kept on ice for 5 min. Lysis was stopped by filling the tubes with cold PBS. Samples were centrifuged again and finally resuspended in 1 mL cold PBS. Viable cells for downstream use for all tissues were counted in a Vi-CELL cell counter (Beckman Coulter) at a 1:60 dilution.

Flow cytometry

Single cell suspensions were first incubated with 1:100 Zombie NIR (L34976, Life Technologies) for 10 min in the dark at room temperature. After a washing step, samples were incubated with 1:100 H-2D(b) Mouse ASMT-NMELM ADPGK PE-conjugated tetramer (TB-5113-1, MBL) for 30 min at room temperature. After washing, surface staining including 1:50 Fc Block (70-0161-U500, Tonbo Biosciences) was performed for 30 min on ice. Cells were fixed using the eBioscience FoxP3 kit

(00-5523-00, Life Technologies) and intracellular staining was added to samples for 30 min on ice before final wash with Fluorescence-Activated Cell Sorting (FACS) buffer (PBS containing 2% FBS and 1 mM EDTA). Samples were run on an LSRFortessa X-50 (Becton Dickinson). Data was analyzed by FlowJo V.10.7 (TreeStar). A detailed list of all antibodies used for flow cytometry can be found in table 1.

Data analysis and statistics

All statistical analyses were performed with GraphPad Prism V.9 and V.10. All data were tested for normality. For single parameter comparisons involving more than two groups from flow cytometry or bioluminescence, one-way analysis of variance (ANOVA) tests adjusted for Tukey's multiple comparisons were applied in data passing normality, while Kruskal-Wallis tests adjusted for Dunn's multiple comparisons were applied for non-parametric data. For Kaplan-Meier survival curve comparisons, log-rank Mantel-Cox tests were applied. For body weight curve comparisons, two-way ANOVA adjusted for Dunn's multiple comparisons was applied. For Kaplan-Meier survival curve comparisons, log-rank Mantel-Cox tests were applied. A p value of 0.05 or less was considered statistically significant. Unless stated otherwise, error bars in plots represent SD and horizontal black bars represent means. Unless stated otherwise, representative data from n=1 of three (subcutaneous) or n=1 of two (systemic) experiments are shown in figure panels. A minimum of three biological replicates were run in all comparisons. All supporting values for data shown in this manuscript are available at online supplemental file 3.

X Marcel Arias-Badia @MarcelArias

Acknowledgements We thank the UCSF Parnassus Flow Cytometry Core PFCC (RRID:SCR_018206) for assistance generating Flow Cytometry data. We also thank the UCSF Preclinical Imaging Core for technical help. We thank Oscar Aguilar and Lewis Lanier at UCSF for providing the backbone vector to generate the Luc-MC38-PSCA cells. We also thank BioRender for digital image support.

Contributors MA-B, AG, JVG, WR and LF conceived the study. MA-B, C-CSP, YML, PC, AS, EM and MT performed experiments and acquired data. MA-B and C-CSP analysed and interpreted data. AG, JVG and WR provided critical reagents. MA-B and LF wrote the initial draft of the manuscript. AG, JVG, WR and LF supervised the research. MA-B, LF, JVG and WR wrote the manuscript. LF is the guarantor of this study.

Funding This study was supported by research funding from AbbVie. AbbVie participated in study design, data acquisition and interpretation, as well as manuscript writing and submission to JITC. LF is supported by NIH R35CA253175. Research reported here was supported in part by the DRC Center Grant NIH P30 DK063720.

Competing interests LF reports research support and consultancy fees from AbbVie to the institution and himself, respectively. LF also reports support from Bavarian Nordic, Bristol-Myers Squibb, Dendreon, Janssen, Merck, Roche/Genentech; ownership interests in Actym, Bioatla, Immunogenesis, Nutcracker, RAPT and Therapaint unrelated to the work here. AG, JVG, EM and WR were employed at AbbVie during the development of this study. The other authors declare no competing interests.

Patient consent for publication Not applicable.

Ethics approval Not applicable.

Provenance and peer review Not commissioned; externally peer reviewed.

Data availability statement Data are available upon reasonable request. All data relevant to the study are included in the article or uploaded as supplementary information.

Supplemental material This content has been supplied by the author(s). It has not been vetted by BMJ Publishing Group Limited (BMJ) and may not have been peer-reviewed. Any opinions or recommendations discussed are solely those of the author(s) and are not endorsed by BMJ. BMJ disclaims all liability and responsibility arising from any reliance placed on the content. Where the content includes any translated material, BMJ does not warrant the accuracy and reliability of the translations (including but not limited to local regulations, clinical guidelines, terminology, drug names and drug dosages), and is not responsible for any error and/or omissions arising from translation and adaptation or otherwise.

Open access This is an open access article distributed in accordance with the Creative Commons Attribution Non Commercial (CC BY-NC 4.0) license, which permits others to distribute, remix, adapt, build upon this work non-commercially, and license their derivative works on different terms, provided the original work is properly cited, appropriate credit is given, any changes made indicated, and the use is non-commercial. See <http://creativecommons.org/licenses/by-nc/4.0/>.

ORCID iD

Marcel Arias-Badia <http://orcid.org/0000-0003-2270-0676>

REFERENCES

- Postow MA, Sidlow R, Hellmann MD, *et al.* Immune-Related Adverse Events Associated with Immune Checkpoint Blockade. *N Engl J Med* 2018;378:158–68.
- Fecher LA, Agarwala SS, Hodi FS, *et al.* Ipilimumab and its toxicities: a multidisciplinary approach. *Oncologist* 2013;18:733–43.
- Galsky MD, Autio KA, Cabanski CR, *et al.* Clinical and Translational Results from PORTER, a Multi-cohort Phase 1 Platform Trial of Combination Immunotherapy in Metastatic Castration-Resistant Prostate Cancer. *Clin Cancer Res* 2025.
- O'Day SJ, Maio M, Chiarion-Sileni V, *et al.* Efficacy and safety of ipilimumab monotherapy in patients with pretreated advanced melanoma: a multicenter single-arm phase II study. *Ann Oncol* 2010;21:1712–7.
- Duerinck J, Schwarze JK, Awada G, *et al.* Intracerebral administration of CTLA-4 and PD-1 immune checkpoint blocking monoclonal antibodies in patients with recurrent glioblastoma: a phase I clinical trial. *J Immunother Cancer* 2021;9:e002296.
- Schwarze JK, Awada G, Cras L, *et al.* Intratumoral Combinatorial Administration of CD1c (BDCA-1)⁺ Myeloid Dendritic Cells Plus Ipilimumab and Avelumab in Combination with Intravenous Low-Dose Nivolumab in Patients with Advanced Solid Tumors: A Phase IB Clinical Trial. *Vaccines (Basel)* 2020;8:670.
- Pai C-C, Simons DM, Lu X, *et al.* Tumor-conditional anti-CTLA4 uncouples antitumor efficacy from immunotherapy-related toxicity. *J Clin Invest* 2019;129:349–63.
- Yadav M, Jhunjhunwala S, Phung QT, *et al.* Predicting immunogenic tumour mutations by combining mass spectrometry and exome sequencing. *Nature New Biol* 2014;515:572–6.
- Casagrande S, Sopetto GB, Bertalot G, *et al.* Immune-Related Adverse Events Due to Cancer Immunotherapy: Immune Mechanisms and Clinical Manifestations. *Cancers (Basel)* 2024;16:1440.
- Allouchery M, Lombard T, Martin M, *et al.* Safety of immune checkpoint inhibitor rechallenge after discontinuation for grade ≥ 2 immune-related adverse events in patients with cancer. *J Immunother Cancer* 2020;8:e001622.
- Marabelle A, Kohrt H, Levy R. Intratumoral anti-CTLA-4 therapy: enhancing efficacy while avoiding toxicity. *Clin Cancer Res* 2013;19:5261–3.
- Marabelle A, Kohrt H, Sagiv-Barfi I, *et al.* Depleting tumor-specific Tregs at a single site eradicates disseminated tumors. *J Clin Invest* 2013;123:2447–63.
- Fransen MF, van der Sluis TC, Ossendorp F, *et al.* Controlled local delivery of CTLA-4 blocking antibody induces CD8⁺ T-cell-dependent tumor eradication and decreases risk of toxic side effects. *Clin Cancer Res* 2013;19:5381–9.
- Francis DM, Manspeaker MP, Schudel A, *et al.* Blockade of immune checkpoints in lymph nodes through locoregional delivery augments cancer immunotherapy. *Sci Transl Med* 2020;12:eaay3575.
- Hebb JPO, Mosley AR, Vences-Catalán F, *et al.* Administration of low-dose combination anti-CTLA4, anti-CD137, and anti-OX40 into murine tumor or proximal to the tumor draining lymph node induces systemic tumor regression. *Cancer Immunol Immunother* 2018;67:47–60.
- van Hooren L, Sandin LC, Moskalev I, *et al.* Local checkpoint inhibition of CTLA-4 as a monotherapy or in combination with anti-PD1 prevents the growth of murine bladder cancer. *Eur J Immunol* 2017;47:385–93.
- Tawbi HA, Forsyth PA, Algazi A, *et al.* Combined Nivolumab and Ipilimumab in Melanoma Metastatic to the Brain. *N Engl J Med* 2018;379:722–30.
- Spitzer MH, Carmi Y, Reticker-Flynn NE, *et al.* Systemic Immunity Is Required for Effective Cancer Immunotherapy. *Cell* 2017;168:487–502.
- Rahim MK, Okholm TLH, Jones KB, *et al.* Dynamic CD8⁺ T cell responses to cancer immunotherapy in human regional lymph nodes are disrupted in metastatic lymph nodes. *Cell* 2023;186:1127–43.
- Fransen MF, Schoonderwoerd M, Knopf P, *et al.* Tumor-draining lymph nodes are pivotal in PD-1/PD-L1 checkpoint therapy. *JCI Insight* 2018;3:e124507.
- Di Giacomo AM, Lahn M, Eggermont AM, *et al.* The future of targeting cytotoxic T-lymphocyte-associated protein-4: Is there a role? *Eur J Cancer* 2024;198:113501.
- Liu M, Wang X, Du X, *et al.* Soluble CTLA-4 mutants ameliorate immune-related adverse events but preserve efficacy of CTLA-4- and PD-1-targeted immunotherapy. *Sci Transl Med* 2023;15:eabm5663.
- Wing K, Onishi Y, Prieto-Martin P, *et al.* CTLA-4 control over Foxp3⁺ regulatory T cell function. *Science* 2008;322:271–5.
- Selby MJ, Engelhardt JJ, Quigley M, *et al.* Anti-CTLA-4 antibodies of IgG2a isotype enhance antitumor activity through reduction of intratumoral regulatory T cells. *Cancer Immunol Res* 2013;1:32–42.
- Lax BM, Palmeri JR, Lutz EA, *et al.* Both intratumoral regulatory T cell depletion and CTLA-4 antagonism are required for maximum efficacy of anti-CTLA-4 antibodies. *Proc Natl Acad Sci USA* 2023;120:e2300895120.
- Brummelman J, Mazza EMC, Alvisi G, *et al.* High-dimensional single cell analysis identifies stem-like cytotoxic CD8⁺ T cells infiltrating human tumors. *J Exp Med* 2018;215:2520–35.
- Siddiqui I, Schaeuble K, Chennupati V, *et al.* Intratumoral Tcf1+PD-1+CD8⁺ T Cells with Stem-like Properties Promote Tumor Control in Response to Vaccination and Checkpoint Blockade Immunotherapy. *Immunity* 2019;50:195–211.